



# CHORUS

This is the accepted manuscript made available via CHORUS. The article has been published as:

## Substrate Clamping Effects on Irreversible Domain Wall Dynamics in Lead Zirconate Titanate Thin Films

F. Griggio, S. Jesse, A. Kumar, O. Ovchinnikov, H. Kim, T. N. Jackson, D. Damjanovic, S. V. Kalinin, and S. Trolier-McKinstry

Phys. Rev. Lett. **108**, 157604 — Published 13 April 2012

DOI: [10.1103/PhysRevLett.108.157604](https://doi.org/10.1103/PhysRevLett.108.157604)

*To be submitted to Phys. Rev. Lett.*

**Substrate Clamping Effects on Irreversible Domain Wall Dynamics in  
Lead Zirconate Titanate Thin Films**

F. Griggio<sup>1</sup>, S. Jesse<sup>2</sup>, A. Kumar<sup>2</sup>, O. Ovchinnikov<sup>2</sup>, H. Kim<sup>3</sup>, T. N. Jackson<sup>3</sup>,  
D. Damjanovic,<sup>4</sup> S. V. Kalinin<sup>2</sup>, S. Trolier-McKinstry<sup>1</sup>

<sup>1</sup>*Materials Research Institute and Materials Science and Engineering Department, Penn State University,  
Materials Research Laboratory, The Pennsylvania State University, University Park, Pennsylvania 16802,  
USA*

<sup>2</sup>*The Center for Nanophase Materials Science, Oak Ridge National Laboratory,  
Oak Ridge, Tennessee 37831, USA*

<sup>3</sup>*Center for Thin Film Devices and Department of Electrical Engineering,  
Electrical Engineering East, University Park, The Pennsylvania State University, Pennsylvania 16802,  
USA*

<sup>4</sup>*Ceramic Laboratory, Swiss Federal Institute of Technology in Lausanne (EPFL),  
CH-1015 Lausanne, Switzerland*

The role of long-range strain interactions on domain wall dynamics is explored through macroscopic and local measurements of nonlinear behavior in mechanically clamped and released polycrystalline lead zirconate-titanate (PZT) films. Released films show a dramatic change in the global dielectric nonlinearity and its frequency

dependence as a function of mechanical clamping. Furthermore, we observe transition from strong clustering of nonlinear response for clamped case to almost uniform nonlinearity for released film. This behavior is ascribed to increased mobility of domain walls. These results suggest the dominant role of collective strain interactions mediated by the local and the global mechanical boundary conditions on the domain wall dynamics. The work presented in this paper demonstrates that measurements on clamped films may considerably underestimate the piezoelectric coefficients and coupling constants of released structures used in microelectromechanical systems, energy harvesting systems, and microrobots.

Strain in epitaxial oxide films has become a universally recognized method for tuning materials properties,<sup>1-3</sup> enabling novel couplings between magnetic, lattice and strain behaviors,<sup>4-6</sup> stabilizing new phases<sup>7</sup> or domain morphologies.<sup>8</sup> Systematic studies of a material's response to strain enable exploration of the fundamental mechanisms responsible for e.g. the ferroelectric instability.<sup>9-12</sup>

While strain effects on intrinsic properties<sup>9,12</sup> and domain morphologies<sup>13,14</sup> are readily amenable to theoretical and experimental studies, their role on local and emergent properties<sup>15</sup> in disordered materials, including polycrystalline ferroelectric films and relaxors, remains virtually unexplored.<sup>16,17</sup> Indeed, many of these materials exhibit unique physical properties including giant electromechanical coupling coefficients, broad dispersions of dielectric permittivity, etc.<sup>18-21</sup> These phenomena are often associated with the presence of nanoscale textures of domains or nanoscale phase separation.<sup>22-24</sup> In all these materials, the dominant order parameter is either strain (ferroelastics) or is strongly coupled to strain (relaxors, morphotropic systems), suggesting the significant role of frustrated or random strain interactions.<sup>25-27</sup> Correspondingly, tuning mechanical boundary conditions can significantly affect emergent behaviors in the disordered ferroics and provide insight on corresponding coupling mechanisms.

Here, we aim to explore domain wall dynamics as reflected in ferroelectric nonlinearities in model  $\text{PbZr}_{0.52}\text{Ti}_{0.48}\text{O}_3$  thin films. In PZT ceramics, domain wall motion may contribute to more than 50% of the dielectric and piezoelectric properties at room temperature.<sup>23,28</sup> However, in thin films these extrinsic contributions to the piezoelectric response can be severely limited by several factors, including substrate clamping.<sup>29</sup> Recent spatially-resolved studies of piezoelectric nonlinearities have demonstrated the

presence of micron-sized clusters of nonlinear activity, suggesting that surprisingly long-range phenomena are responsible for nonlinear interactions (at a length scale significantly larger than the grain size or domain size). Here, we aim to explore the role of long-range elastic interactions on electro-mechanical response through a combination of local and macroscopic measurements of nonlinearity in clamped and mechanically released PZT films. The nonlinearity is analyzed using Rayleigh relations<sup>30</sup> and corresponding frequency dispersions.<sup>31</sup>

In order to release the PZT film from the underlying substrate, diaphragm structures were fabricated according to the schematic in Figure 1 (a, b). The effect of mechanical boundary conditions on dielectric nonlinearity is shown in Figure 1 (c, d). The electric field dependence of the dielectric constant,  $\epsilon_r$ , and the minor polarization hysteresis loops for diaphragm structures were measured before and after cracking the diaphragms.<sup>32</sup> When the diaphragms were broken, the three sections of the diaphragm curled up by 430 nm due to the release of the tensile stress in the PZT layer over 11.4% of the measured capacitor area. As a result, the irreversible Rayleigh coefficient  $\alpha_\epsilon$ , which indicates the irreversible motion of domain walls,<sup>33</sup> increased by 114 %, rising from  $12.7 \pm 0.04$  cm/kV up to  $27.2 \pm 0.07$  cm/kV. Using a parallel capacitor model, the Rayleigh parameters were determined for fully released and partially released PZT, as shown in Table 1.

INSERT FIG. 1 AND TABLE 1

Both fitting errors for the Rayleigh parameters and errors in the released area were accounted for in the error propagation. It was found that  $\alpha_\varepsilon$  of the released and broken area increased by one order of magnitude, reaching values comparable to that of undoped morphotropic phase boundary PZT bulk ceramics. For the PZT diaphragm which was released from the Si substrate but not broken,  $\alpha_\varepsilon$  increased by 75 %.<sup>32</sup>

To gain further insight into strain effect on dielectric nonlinearity, the frequency dispersion of the Rayleigh parameters was ascertained as shown in Fig. 2.

INSERT FIG. 2

Although the Rayleigh model by itself does not have any time dependence, in random systems controlled by a normal distribution of restoring forces, the extrinsic contributions often follow a logarithmic frequency dependence over a broad frequency range below so-called microwave region and above mHz- Hz range.<sup>34-36</sup>

$$\varepsilon'_{init}(\omega) = e_0 + e \ln\left(\frac{1}{\omega}\right) \quad (1)$$

$$\alpha'_\varepsilon(\omega) = a_0 + a \ln\left(\frac{1}{\omega}\right) \quad (2)$$

where  $\varepsilon'_{init}$  and  $\alpha'_\varepsilon$  are reversible and irreversible Rayleigh coefficients<sup>30</sup> respectively. Defining the  $a/a_0$  ratio as frequency attenuation factor of the irreversible Rayleigh coefficient, it was found that partially released capacitors have a weaker attenuation than clamped ones, with a decrease in  $\alpha'_\varepsilon$  of 120 % over the 800 Hz – 1 MHz frequency range (see Table 1).

As previously described by Bassiri-Gharb *et al.*, the stronger frequency dependence of  $\alpha'_\epsilon$  for the completely clamped capacitors is indicative of a larger number of irreversible jumps of domain walls freezing out at higher frequencies.<sup>37</sup> Interestingly enough, a different trend was observed for the extrinsic reversible frequency attenuation factor  $e/e_0$ , with a slower decay with frequency for the completely clamped samples. This could be due to a larger population of domain walls contributing reversibly in the clamped films up to higher frequencies. Both observations would be consistent with the assumption that the barrier heights associated with specific pinning centers rise under clamping.

A few key points should be considered in interpreting these results. First, the concentration of microstructure-based pinning sites and those of chemical origin (vacancies, impurities) is comparable between the released and clamped capacitors. Moreover, on undercutting the Si, the *average* residual stress in the PZT film changes only a small amount, as the diaphragm stays taut, with only small vertical deflections observed near the central hole. Thus, the observed differences in the Rayleigh response on releasing the sample from the underlying substrate are likely to be related, at least in part, to a change in the *local* stresses and the bending rigidity of the *structure* as illustrated in Figure 3.

INSERT FIG. 3

Secondly, it is clear that the dielectric nonlinearities change substantially when both the local and the average residual stresses are reduced in the film, when the released diaphragm is broken. The large irreversible Rayleigh constant observed in this case is

comparable to those of bulk ceramics, and exceeds those of the clamped film by an order of magnitude. This points to the fact that one of the most significant factors reducing the irreversible motion of domain walls in PZT films on Si is a combination of residual stress and the substrate rigidity. The temperatures utilized throughout the release process were low, and are not expected to perturb the domain state significantly. However, because the samples were poled following release, there is a chance that the domain state changed during the poling process. In general, however, a reduction in the domain wall density would be expected during poling. Following release, however, the dielectric and piezoelectric nonlinearities *rise*, demonstrating that the wall mobility must increase substantially, if the domain wall density has indeed dropped.

To gain insight into spatially resolved nonlinear behavior, band excitation piezoresponse force microscopy (BE-PFM) was employed to characterize the *local* converse piezoelectric response.<sup>38</sup> The bias dependence of  $A_{max}$  allows effective piezoelectric coefficient,  $d_{33,init}$ , and Rayleigh coefficient,  $\alpha_d$ , to be determined. Note that while  $\alpha_d$  and  $d_{33,init}$  are dependent on microscope calibration, the ratio is measured in absolute units.

Figure 4 shows the spatially resolved maps of topography, resonance frequency  $\omega_0$ , phase at  $\omega_0$  averaged over the amplitude modulation and the standard deviation of the resonance frequency as a function of  $V_{ac}$  across the clamped/released boundary.

INSERT FIG. 4

By using the BE method to decouple voltage changes of  $\omega_0$  and response amplitude, it is possible to exclude the presence of surface cross-talk or tip-surface junction nonlinearity. In the released area, the changes in resonance frequency were as high as 15 kHz and are not a result of dynamic nonlinearities,<sup>39</sup> since no softening was observed in the standard deviation of  $\omega_0(V_{ac})$  map reported in Figure 4 (d). It is speculated that this may be due to local variations in the mechanical boundary conditions, perhaps from an incompletely circular membrane, or residual Si on the back of some of the diaphragm.

A phase change was detected in BE-PFM maps of the same area average over the  $V_{ac}$  excitation range. This phase change may be related to a contribution from a pitching mode of the actuated diaphragm.

The standard deviation of  $\omega_0(V_{ac})$  map is below 200 Hz for most of the map, which is an indication of negligible dynamic nonlinearities, considering that the peak width at the maximum  $V_{ac}$  is 5 kHz; however regions showing softening of the resonance peak as a function of the applied excitation voltage are apparent in the clamped half of the explored area.<sup>38</sup> The local dynamic nonlinearities present in those regions increased the noise in the  $\alpha_d / d_{33,init}$  map and prevented a quantitative characterization. The following statistical analysis on local  $\alpha_d / d_{33,init}$  values did not include those areas.

In Figure 5 (b) and (c), the histograms of nonlinear response relative to clamped and released regions are compared; spatial averages of  $0.002 \pm 0.010$  cm/kV and  $0.013 \pm 0.006$  cm/kV were characterized for the clamped and released regions, the latter being very close to the dielectric nonlinearity value characterized on completely clamped capacitors of the sample. This would indicate that the same population of domain walls

responding to the exciting field globally in dielectric measurements can be probed at much smaller volumes ( $\sim 0.022 \mu\text{m}^3$ ) when the diaphragms are released.<sup>40,41</sup>

Potential contributions to the differences in domain wall motion between the clamped and released regions include a partial release of the average residual in-plane tensile stress due to the thermal expansion coefficient mismatch between the PZT and the Si substrate. This was manifested by the small amount of vertical deflection observed after release. Also, deformation strains, associated with formation of domains, would be expected to couple mechanically to the substrate rigidity. This, in turn, will produce local stresses at the PZT-Pt interface which differ from the average residual stress. Such local mechanical stresses are expected to influence the configuration and mobility of domain walls at the PZT-Pt interface.

INSERT FIG. 5

The local piezoelectric nonlinearity data suggest that a larger fraction of domain walls is contributing irreversibly to the piezoelectric properties in the released (but not broken) region of the PZT. This is consistent with the measured frequency dispersion of the dielectric Rayleigh parameters. It is also critical to note that the length scale over which correlated motion of domain walls is observed increases substantially as the diaphragm is released. Thus, while strong clustering of the  $\alpha_d / d_{33,init}$  ratio is observed in the clamped region, this clustering largely disappears in the released portion of the sample. This observation was borne out on larger areas of the released portion of the

sample, as shown in Figure 5. The histogram of the  $\alpha_d / d_{33,init}$  ratio on this portion of the sample shows a much tighter distribution than is characteristic of the clamped regions.

It cannot be excluded that a resonating mode of the diaphragm structure may influence the local response collected by the AFM cantilever. It is hypothesized that in this scenario the structure nonlinearity would add an offset, but would preserve the same clustering characterized in the clamped capacitors. However, the spatial distributions observed for the clamped and released regions (Fig. 5 (b)) showed a significant change, with a much narrower distribution of  $\alpha_d / d_{33,init}$  values characterized in the released region.

Thus, it is believed that the observed increase in the dielectric  $\alpha_e / \epsilon_{init}$  measured for the released and broken region, is related to the larger volume of film over which correlated motion of domain walls can occur. This, in turn, is believed to result from the fact that reduction of local stresses on removal of the substrate may eliminate pinning centers at the film/electrode interface. Therefore, this description is consistent with the piezoelectric nonlinearity being a function of the dynamic coupling between domain walls and the length-scale of the interaction being influenced dramatically by *local* stresses.

To summarize, the influence of mechanical boundary conditions was analyzed in morphotropic phase boundary PZT thin films on Si substrates. By creating cavities beneath the PZT capacitors, the mechanical boundary conditions were altered and the domain wall motion contributions were probed dielectrically and piezoelectrically as a function of the mechanical boundary conditions.

When the piezoelectric nonlinear measurements were performed on released regions of PZT, a remarkable difference in the length scale of cooperative interaction was observed. This change was consistent with a smaller dispersion of the irreversible contributions to the dielectric constant in partially released samples. These results offer evidence for a significant influence of substrate clamping on the extrinsic contributions to the dielectric and piezoelectric properties, and the length scale over which such changes are manifested. Given that most piezoelectric microelectromechanical systems utilize partially or fully released structures, the results have significant implications for miniaturized sensors, actuators, transducers, and energy harvesting systems.<sup>42,43</sup> It is worth noting that substrate clamping and mobile interfaces interaction is a cross-cutting phenomenon, of interest in other physical system such as ferromagnetic and ferroelastic materials and systems undergoing martensitic transformations.

### **Acknowledgments**

Support for this work was provided in part by the National Security Science and Engineering Faculty Fellowship and by CNMS user proposal CNMS2010-090 (FG and STM). A portion of this research was conducted at the Center for Nanophase Materials Sciences, which is sponsored at Oak Ridge National Laboratory by the Office of Basic Energy Sciences, U.S. Department of Energy.

## References

- 1 D. G. Schlom, L. Q. Chen, C. B. Eom, K. M. Rabe, S. K. Streiffer, and J. M.  
Triscone, in *Annual Review of Materials Research*; Vol. 37 (2007), p. 589.
- 2 A. Rivera-Calzada, M. R. Diaz-Guillen, O. J. Dura, G. Sanchez-Santolino, T. J.  
Pennycook, R. Schmidt, F. Y. Bruno, J. Garcia-Barriocanal, Z. Sefrioui, N. M.  
Nemes, M. Garcia-Hernandez, M. Varela, C. Leon, S. T. Pantelides, S. J.  
Pennycook, and J. Santamaria, *Advanced Materials* **23**, 5268 (2011).
- 3 J. M. Rondinelli and N. A. Spaldin, *Advanced Materials* **23**, 3363 (2011).
- 4 C. W. Nan, M. I. Bichurin, S. X. Dong, D. Viehland, and G. Srinivasan, *J. Appl.*  
*Phys.* **103**, 031101 (2008).
- 5 G. Catalan, A. Lubk, A. H. G. Vlooswijk, E. Snoeck, C. Magen, A. Janssens, G.  
Rispens, G. Rijnders, D. H. A. Blank, and B. Noheda, *Nat. Mater.* **10**, 963 (2011).
- 6 A. Scholl, J. Stohr, J. Luning, J. W. Seo, J. Fompeyrine, H. Siegwart, J. P.  
Locquet, F. Nolting, S. Anders, E. E. Fullerton, M. R. Scheinfein, and H. A.  
Padmore, *Science* **287**, 1014 (2000).
- 7 R. J. Zeches, M. D. Rossell, J. X. Zhang, A. J. Hatt, Q. He, C. H. Yang, A. Kumar,  
C. H. Wang, A. Melville, C. Adamo, G. Sheng, Y. H. Chu, J. F. Ihlefeld, R. Erni,  
C. Ederer, V. Gopalan, L. Q. Chen, D. G. Schlom, N. A. Spaldin, L. W. Martin,  
and R. Ramesh, *Science* **326**, 977 (2009).
- 8 J. S. Speck and W. Pompe, *J. Appl. Phys.* **76**, 466 (1994).
- 9 K. M. Rabe, *Current Opinion in Solid State & Materials Science* **9**, 122 (2006).
- 10 C. Ederer and N. A. Spaldin, *Phys. Rev. Lett.* **95**, 257601 (2005).
- 11 M. Dawber, K. M. Rabe, and J. F. Scott, *Reviews of Modern Physics* **77**, 1083  
(2005).
- 12 S. Picozzi and C. Ederer, *J. Phys. Condens. Matter* **21**, 303201 (2009).
- 13 S. Choudhury, Y. L. Li, C. E. Krill, and L. Q. Chen, *Acta Mater.* **53**, 5313 (2005).
- 14 G. Sheng, J. X. Zhang, Y. L. Li, S. Choudhury, Q. X. Jia, Z. K. Liu, and L. Q.  
Chen, *Appl. Phys. Lett.* **93**, 232904 (2008).
- 15 Basic Energy Sciences Advisory Committee (BESAC) Grand Challenges report.  
Available at: <http://science.energy.gov/bes/news-and-resources/reports/abstracts/-GC>.
- 16 M. Tyunina and J. Levoska, *Phys. Rev. B: Condens. Matter* **65**, 132101 (2002).
- 17 M. Tyunina and J. Levoska, *Phys. Rev. B: Condens. Matter* **72**, 104112 (2005).
- 18 S. E. Park and T. R. ShROUT, *J. Appl. Phys.* **82**, 1804 (1997).
- 19 C. Stock, L. Van Eijck, P. Fouquet, M. Maccarini, P. M. Gehring, G. Xu, H. Luo,  
X. Zhao, J. F. Li, and D. Viehland, *Phys. Rev. B: Condens. Matter* **81**, 144127  
(2010).
- 20 A. A. Bokov and Z. G. Ye, *J. Mater. Sci.* **41**, 31 (2006).
- 21 N. Setter, D. Damjanovic, L. Eng, G. Fox, S. Gevorgian, S. Hong, A. Kingon, H.  
Kohlstedt, N. Y. Park, G. B. Stephenson, I. Stolitchnov, A. K. TagansteV, D. V.  
Taylor, T. Yamada, and S. Streiffer, *J. Appl. Phys.* **100**, 051606 (2006).
- 22 D. Zekria, V. A. Shuvaeva, and A. M. Glazer, *J. Phys. Condens. Matter* **17**, 1593  
(2005).
- 23 R. E. Eitel, T. R. ShROUT, and C. A. Randall, *J. Appl. Phys.* **99**, 124110 (2006).

- 24 T. Scholz, B. Mihailova, G. A. Schneider, N. Pagels, J. Heck, T. Malcherek, R. P.  
Fernandes, V. Marinova, M. Gospodinov, and U. Bismayer, *J. Appl. Phys.* **106**,  
074108 (2009).
- 25 T. Lookman, S. R. Shenoy, K. O. Rasmussen, A. Saxena, and A. R. Bishop, *Phys.*  
*Rev. B: Condens. Matter* **67**, 024114 (2003).
- 26 J. Barre, A. R. Bishop, T. Lookman, and A. Saxena, *Phys. Rev. B: Condens.*  
*Matter* **74**, 024104 (2006).
- 27 A. Bussmann-Holder, A. R. Bishop, and T. Egami, *Europhysics Letters* **71**, 249  
(2005).
- 28 A. Pramanick, D. Damjanovic, J. C. Nino, and J. L. Jones, *J. Am. Ceram. Soc.* **92**,  
2291 (2009).
- 29 N. Bassiri-Gharb, I. Fujii, E. Hong, S. Trolier-McKinstry, D. V. Taylor, and D.  
Damjanovic, *J. Electroceram.* **19**, 47 (2007).
- 30 J. W. Lord Rayleigh, *Phil. Mag.* **5**, 225 (1887).
- 31 D. V. Taylor and D. Damjanovic, *J. Appl. Phys.* **82**, 1973 (1997).
- 32 See Supplemental Material at [URL will be inserted by the publisher] for further  
details on samples' preparation and nonlinear characterization.
- 33 D. Damjanovic and M. Demartin, *J. Phys. Condens. Matter* **9**, 4943 (1997).
- 34 M. I. Tsindlekht, G. I. Leviev, V. M. Genkin, I. Felner, Y. B. Paderno, and V. B.  
Filippov, *Phys. Rev. B: Condens. Matter* **73**, 104507 (2006).
- 35 X. B. Wang and P. Ryan, *J. Appl. Phys.* **108**, 083913 (2010).
- 36 D. Damjanovic, *Phys. Rev. B: Condens. Matter* **55**, R649 (1997).
- 37 N. B. Gharb, S. Trolier-McKinstry, and D. Damjanovic, *J. Appl. Phys.* **100**,  
044107 (2006).
- 38 S. Jesse, S. V. Kalinin, R. Proksch, A. P. Baddorf, and B. J. Rodriguez,  
*Nanotechnology* **18**, 435503 (2007).
- 39 F. Griggio, S. Jesse, A. Kumar, D. M. Marincel, D. S. Tinberg, S. V. Kalinin, and  
S. Trolier-McKinstry, *Appl. Phys. Lett.* **98**, 212901 (2011).
- 40 P. Bintachitt, S. Jesse, D. Damjanovic, Y. Han, I. M. Reaney, S. Trolier-  
McKinstry, and S. V. Kalinin, *Proc. Nat. Acad. Sci.* **107**, 7219 (2010).
- 41 B. A. Tuttle, J. A. Voigt, T. J. Garino, D. C. Goodnow, R. W. Schwartz, D. L.  
Lamppa, T. J. Headley, and M. O. Eatough, *Proc. IEEE Int. Symp. Appl.*  
*Ferroelectr.*, 344 (1992).
- 42 S. H. Baek, J. Park, D. M. Kim, V. A. Aksyuk, R. R. Das, S. D. Bu, D. A. Felker,  
J. Lettieri, V. Vaithyanathan, S. S. N. Bharadwaja, N. Bassiri-Gharb, Y. B. Chen,  
H. P. Sun, C. M. Folkman, H. W. Jang, D. J. Kreft, S. K. Streiffer, R. Ramesh, X.  
Q. Pan, S. Trolier-McKinstry, D. G. Schlom, M. S. Rzchowski, R. H. Blick, and  
C. B. Eom, *Science* **334**, 958 (2011).
- 43 S. Trolier-McKinstry, F. Griggio, C. Yaeger, P. Jousse, D. Zhao, S. S. N.  
Bharadwaja, T. N. Jackson, S. Jesse, S. V. Kalinin, and K. Wasa, *IEEE Trans.*  
*Ultrason. Ferroelectr. Freq. Control* **58**, 1782 (2011).

## TABLES

Table I: Summary of the dielectric nonlinearity and logarithmic frequency dependence parameters for the permittivity for clamped, released and released and broken samples.<sup>32</sup>

\* Normalized with respect to the released area. The errors refer to fitting errors.

	$\alpha_e / \epsilon_{inir} \times 10^3$ (kV/cm)	$a/a_0$	$e/e_0$
Clamped	$11.7 \pm 0.04$	$0.033 \pm 0.0004$	$0.010 \pm 0.0004$
Released and broken, normalized*	$103.6 \pm 15.6$	-	-
Released, normalized*	$11.0 \pm 1.8$	$0.015 \pm 0.004$	$0.015 \pm 0.0007$

FIGURES

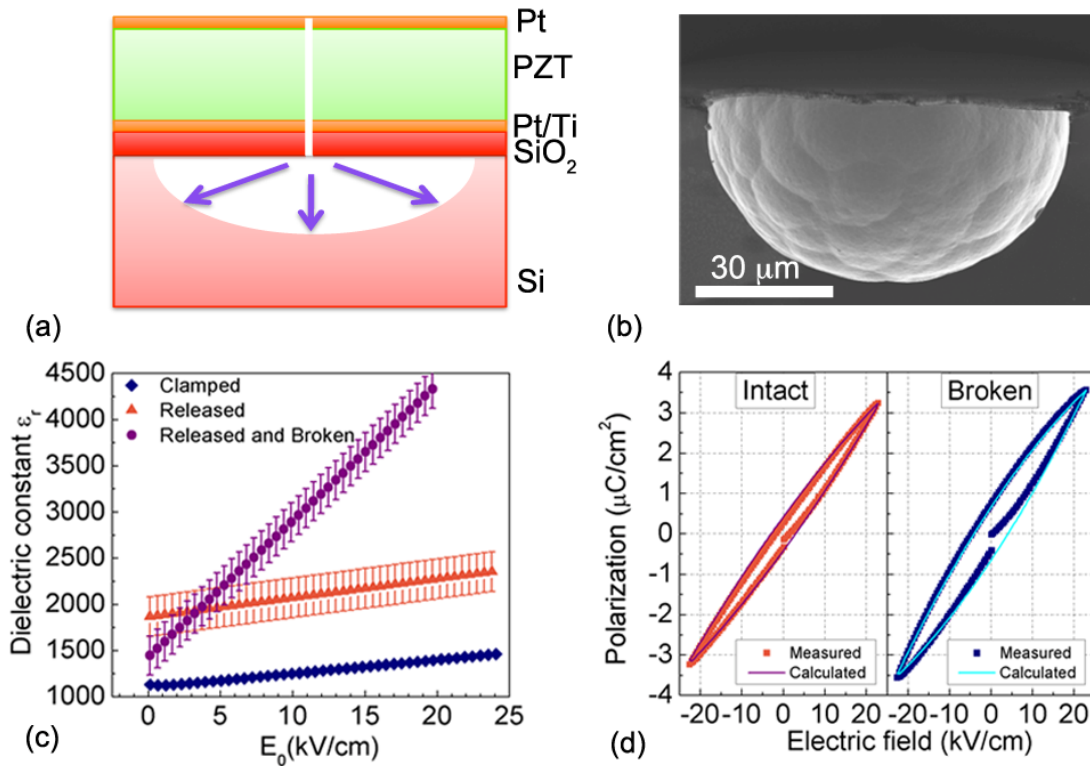


FIG. 1: (Color online) (a) Fabrication process of the diaphragm structures. Dry-etch steps define the top electrode features and openings down to Si and bottom electrode. Isotropic etch using XeF<sub>2</sub> releases the actuator. (b) SEM image of a cross section of fabricated device. (c) Field dependence of the real dielectric permittivity for the fully clamped PZT capacitor, for the fully released PZT and for the fully released and broken PZT capacitor. The orange and violet data points were obtained by normalizing for the released region using a parallel capacitor model. (d) Calculated and measured minor hysteresis loops (uncorrected for the area fraction which was released).

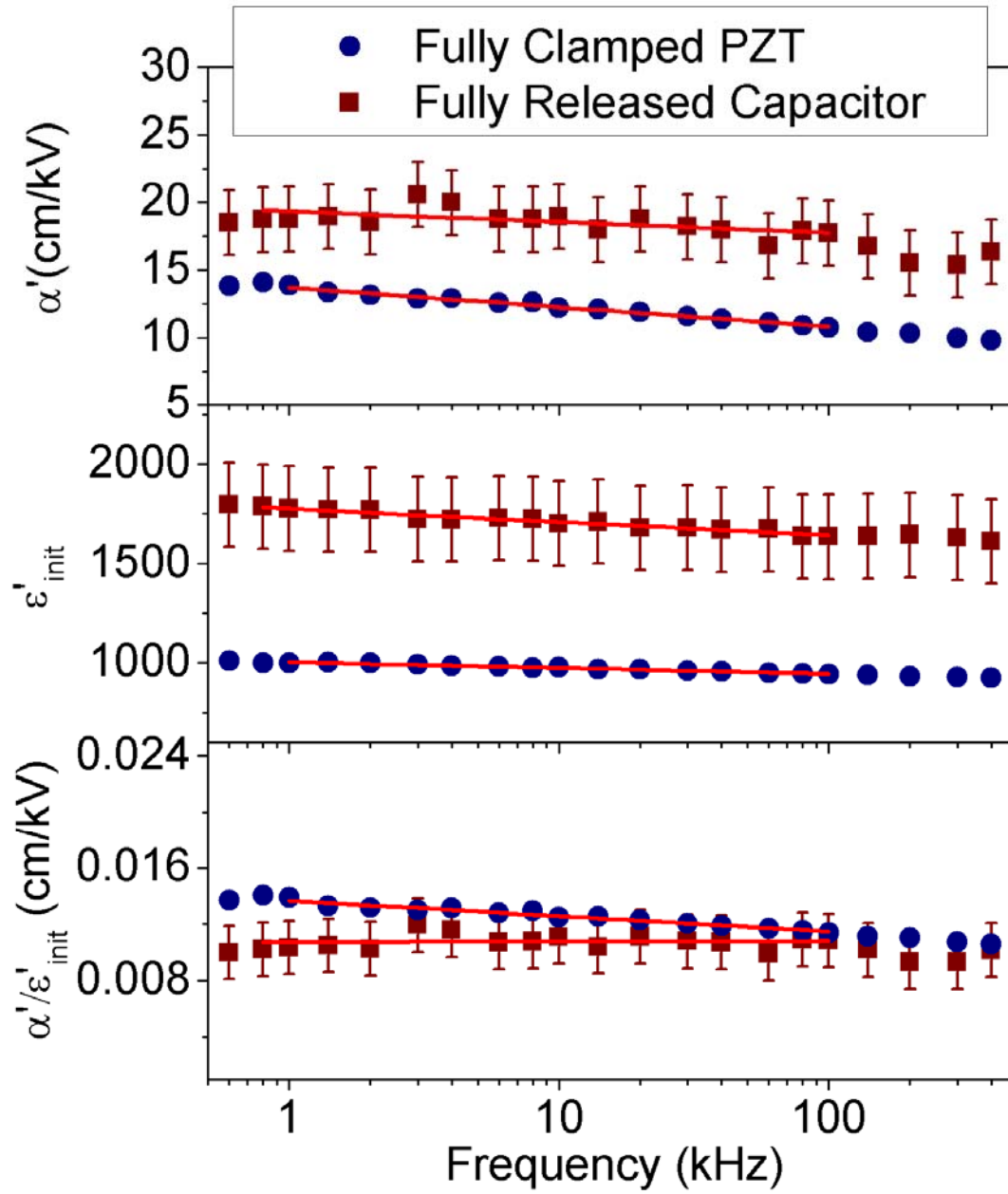


FIG. 2: (Color online) Frequency dispersion of the Rayleigh parameters extrapolated from the AC field dependence of the dielectric constant for clamped capacitors and released but still intact electrodes. The square data points are normalized Rayleigh

parameters from 14 % released areas using a parallel capacitor model. The error bars take into account errors from the area and Rayleigh parameters fittings.

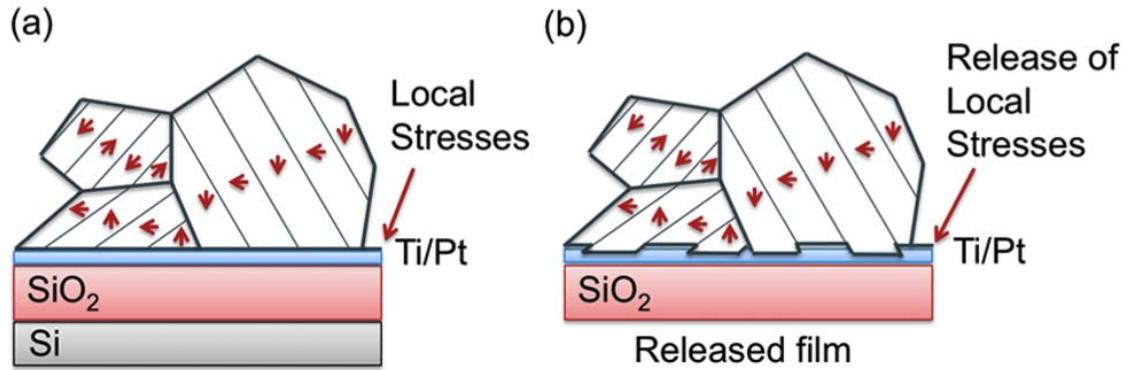


FIG. 3: (Color online) Deformation strains associated with formation of domains could couple mechanically to the underlying substrate. (a) Local stresses develop at the PZT – bottom electrode interface which may differ from the average residual stress and influence the domain wall mobility. (b) Removal of mechanical constraints imposed by the Si substrate at the PZT –bottom electrode interface allows the domain walls to respond to the electric field more freely.

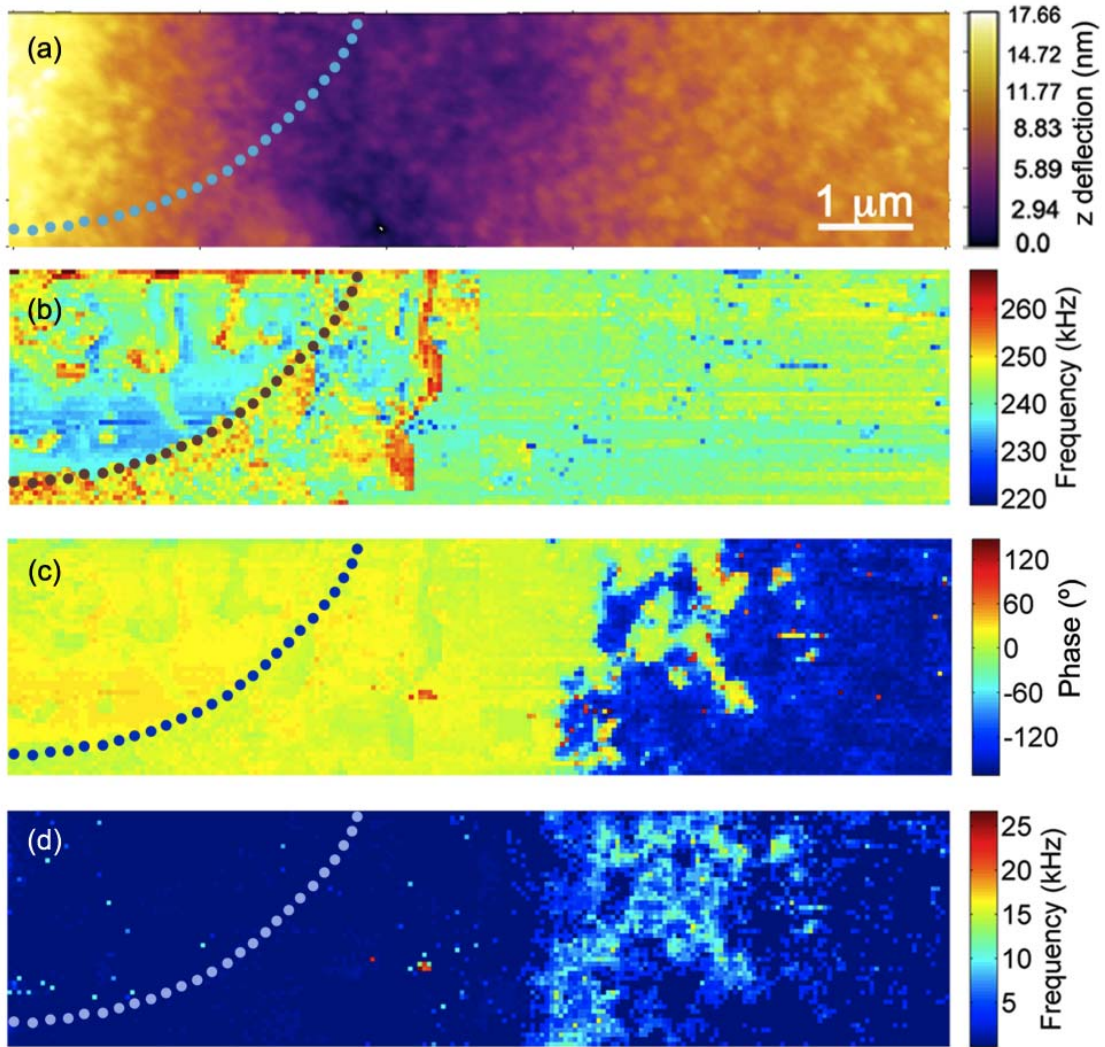


FIG. 4: (Color online) (a) Topography map (b) resonance frequency  $\omega_0$  map, (c) phase at  $\omega_0$  averaged over  $V_{ac}$  and (d) standard deviation of  $\omega_0(V_{ac})$ . The dotted line indicates the clamped-released boundary.

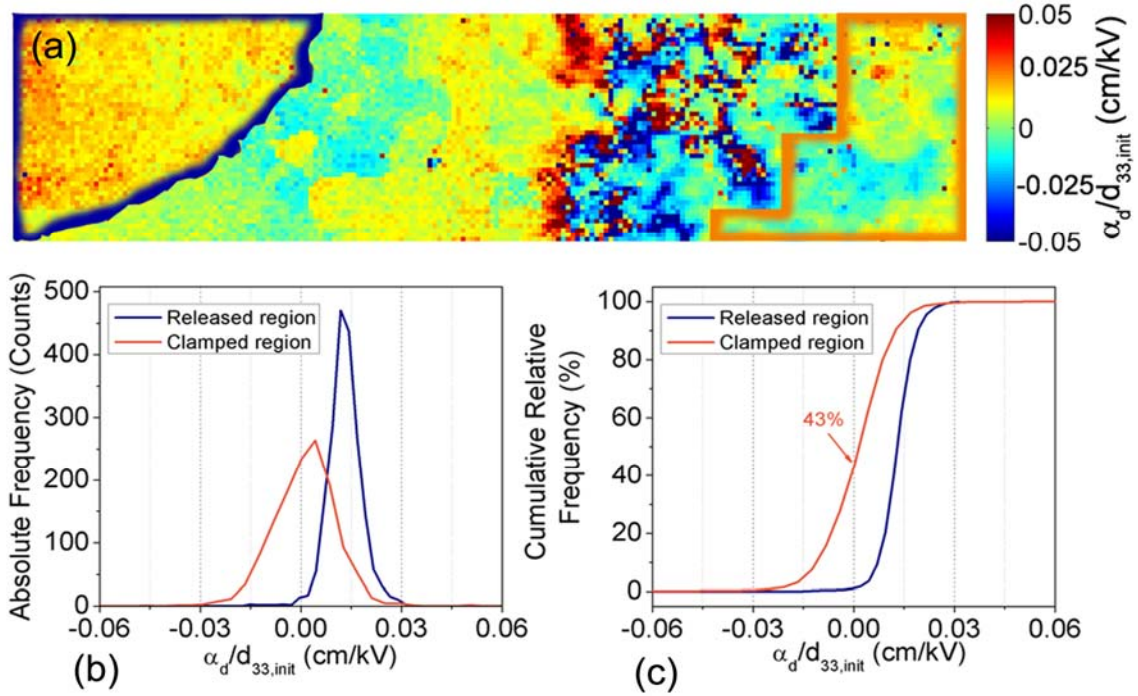


FIG. 5: (Color online) Dependence of nonlinearity on mechanical boundary condition.

(a)  $\alpha_d / d_{33,init}$  ratio map highlighting the released (blue) and clamped (orange) regions used for (b) the absolute frequency and (c) cumulative relative frequency histograms.